

# COMPUTATIONAL FLUID DYNAMICS (CFD) VALIDATION FOR ELECTRIC AND CONVENTIONAL VEHICLE FIRES IN A TUNNEL

Alan Chan Teck Wai<sup>\*1</sup>, Thomas Shean Yaw Choong<sup>1,2</sup>, Mohd Zahirasri bin Mohd Tohir<sup>1</sup>, Mus'ab Abdul Razak<sup>1</sup>

<sup>1</sup>Department of Chemical and Environmental Engineering, Faculty of Engineering, Universiti Putra Malaysia, 43400 Serdang, Selangor, Malaysia

<sup>2</sup>School of Energy and Chemical Engineering, Xiamen University Malaysia, Selangor Darul Ehsan 43900, Malaysia

\*Corresponding author: gs69678@student.upm.edu.my

## Article History

Received:  
November 7th, 2025

Received in revised form:  
January 31st, 2026

Accepted:  
January 31st, 2026

Published:  
June 15th, 2026

## ABSTRACT

This study justifies the application of a Computational Fluid Dynamics (CFD) model, developed using Fire Dynamics Simulator (FDS), for validating and extending the analysis of experimental data from full-scale tunnel fires involving battery electric vehicles (BEVs) and internal combustion engine vehicles (ICEVs). The model was rigorously calibrated using experimental heat release rate (HRR) data and demonstrated a strong capability to reproduce the where and when temperature trends observed across multiple fire scenarios. Quantitative validation through Root Mean Square Error (RMSE) analysis confirmed acceptable engineering accuracy, with contextualized percentage errors providing clear boundaries of model performance. Notably, the model performed with higher accuracy for ICEV fires (~12% error) compared to BEV fires (~20-26% error), highlighting the increased complexity of battery fire dynamics. The CFD model successfully captured critical fire dynamics, including thermal stratification and decay patterns with distance from the fire source. This work establishes that the validated CFD model serves as a reliable and cost-effective tool for supplementing physical experiments, enabling detailed analysis of fire behavior and supporting tunnel safety design where experimental data is limited. The validation is limited to gas temperature predictions in a single tunnel geometry, using experimentally measured HRR as the prescribed fire source together with simplified combustion and material models. The model does not resolve detailed species concentrations or battery degradation chemistry. The reported error ranges (approximately 11–15% for ICEVs and 20–26% for BEVs) should therefore be interpreted as engineering accuracy bounds for similar tunnel configurations, rather than as universal performance indicators.

**Keywords:** Battery Electric Vehicle, Internal Combustion Engine Vehicle, Computational Fluid Dynamics, Root Mean Square Error, Fire Size, Temperature.

## 1.0 INTRODUCTION

The rapid adoption of battery electric vehicles (BEVs) presents unique fire safety challenges in tunnels, distinct from those of conventional internal combustion engine vehicles (ICEVs). Lithium-ion battery fires, driven by thermal runaway, are characterized by intense, sustained heat release and the generation of toxic gases. While full-scale experimental testing provides invaluable benchmark data, its high cost, logistical complexity, and limited sensor coverage result in discrete data points rather than a complete spatiotemporal picture of fire dynamics. Computational Fluid Dynamics (CFD) offers a powerful complementary approach, enabling detailed investigation of fire behavior, smoke propagation, and gas distribution. However, the predictive accuracy of CFD is contingent upon rigorous validation against high-quality experimental data. This study addresses a critical gap in the literature by presenting a systematic, quantitative validation of a CFD model against full-scale BEV and ICEV tunnel fire tests from a 2018 Austrian government research project conducted at the "Zentrum am Berg" facility [1]. A key differentiator of our methodology is the direct use of experimental heat release rate (HRR) data from these tests as the fire source input. This approach isolates the model's fluid dynamics

and heat transfer predictions for validation, independent of combustion modeling uncertainties. The validated model demonstrates a strong capability to replicate measured temperature distributions and fire behavior, establishing its credibility as a "digital twin" for parametric studies, safety system design, and risk assessment. Consequently, this work establishes a rigorously validated, cost-effective CFD framework that can supplement physical testing and enhance fire protection strategies for emerging BEV hazards in tunnel environments.

The scope of the present validation is deliberately restricted to the thermal response (gas temperature) in a straight road tunnel of the Zentrum am Berg geometry, under the specific ventilation, vehicle and HRR conditions reported in the 2018 Austrian test series. The CFD model is driven by the measured HRR curves and does not attempt to predict HRR or gas species, nor does it resolve detailed battery degradation or hydrocarbon combustion chemistry. The quantified RMSE and percentage error values therefore characterise the model's accuracy for reproducing temperatures in this class of full-scale tunnel vehicle fires and are intended to define practical performance bounds for engineering use, rather than to claim universal predictive capability for all tunnel and vehicle configurations.

## **1.1 Literature Review**

This literature review critically examines the current state of research on fire safety modeling for tunnel environments, with particular emphasis on CFD applications. To provide clarity and depth, the review is organized into three core thematic areas: CFD modeling techniques and their application specifically in tunnel fire scenarios; methodologies employed for rigorous validation and benchmarking of CFD simulations against experimental data; and the unique fire behavior characteristics and modeling challenges associated with BEV fires prevalent in modern tunnel safety concerns. This structured approach enables a comprehensive understanding of existing knowledge, prevailing challenges, and research gaps that motivate the present study.

The role of CFD in simulating tunnel fires is well established. CFD models have been extensively applied to analyze temperature distributions, smoke movement, and ventilation behavior in tunnel environments. Studies such as Woodburn (1996) [4] and Reszka et al. (2007) [8] have demonstrated the sensitivity of CFD predictions to ventilation velocity, turbulence modeling, and heat release rates, capturing critical phenomena like smoke layer formation and stratification. Advanced CFD tools, including Fire Dynamics Simulator (FDS), apply detailed turbulence and combustion sub-models to replicate complex fire scenarios in tunnel geometries, enabling detailed thermal and fluid dynamic assessments. These efforts underscore the potential of CFD to provide predictive insights, although challenges remain in achieving precise correlations with experimental data due to flow complexity and transient conditions.

Validation of CFD models through comparison with controlled experimental data is identified as a critical step for establishing predictive reliability in fire safety science. Multiple approaches have been used to benchmark CFD predictions against full-scale and model-scale fire tests, including metrics such as Root Mean Square Error (RMSE) and percentage error relative to peak experimental temperatures. Research emphasizes recurring validation challenges involving turbulence modeling, boundary condition assumptions, grid resolution effects, and measurement uncertainties. Successful validations, such as by Kashef et al. (NRC Canada) [3], link CFD outcomes with risk assessments, enhancing confidence in models for engineering design. Literature highlights the importance of systematic, quantitative validation to not only verify model fidelity but also to understand limitations inherent in approximating complex combustion and radiation phenomena.

In recent years (2020–2024), several experimental and review studies have further characterised lithium-ion battery fire behaviour and EV fire safety in confined infrastructures, including tunnels and underground traffic areas, demonstrating higher peak HRRs, prolonged burning durations and complex combustion gas emission profiles compared with conventional ICEV fires. These works include full-scale tunnel fire tests with BEVs and large-scale EV battery fire experiments with detailed HRR and gas measurements [19,20,21,22]. In parallel, updated CFD studies and validation case studies for tunnel fire and ventilation analysis have emphasised best practices such as using experimentally derived HRR inputs, performing mesh-sensitivity checks and adopting quantitative error metrics (e.g. RMSE, bias) to assess model performance for design applications [23,24]. These more recent contributions underline both the challenges and the necessity of robust CFD validation for EV-related tunnel fires and support the methodology adopted in the present work, which combines full-scale BEV and ICEV tunnel tests with systematic, HRR-driven FDS simulations

Electrification of vehicles introduces unique fire hazards, notably through thermal runaway in lithium-ion batteries, resulting in intense, prolonged fire events with distinctive heat release and toxic emission profiles. Research increasingly focuses on modeling these EV fire dynamics within tunnel environments, recognizing the inadequacy of conventional combustion models to fully capture battery fire behavior. Experimental studies reveal higher peak heat release rates and sustained burning in BEV fires compared to ICEVs, posing challenges for CFD simulation. Integrating battery-specific combustion chemistry into CFD remains an area of active investigation, with ongoing efforts to develop validated numerical models that inform ventilation system design, evacuation strategies, and fire protection measures specific to electric vehicle fires.

## **1.2 Objective**

Collectively, these literature review studies establish CFD as an indispensable tool for tunnel fire safety engineering, capable of detailed analysis of fire dynamics under various scenarios. However, a notable gap persists in robust,

quantitative validation methodologies that use experimentally measured heat release rate (HRR) data from full-scale BEV and ICEV fire tests as direct inputs to CFD models. Existing literature predominantly focuses on predicting fire behavior or validating isolated fire parameters, often lacking a systematic approach that directly ties comprehensive experimental HRR data to temperature validation. This study addresses this gap by employing a rigorous process where experimental HRR serves as the primary fire source input, and the resulting CFD temperature output is quantitatively compared against spatially and temporally resolved experimental temperature datasets. This approach bridges discrete experimental measurements with continuous CFD predictions, thereby enhancing the reliability and engineering applicability of CFD for evaluating complex vehicle fires in tunnel environments. The validated CFD approach aims to provide a reliable and cost-effective tool for fire safety analysis, supporting risk assessment, emergency response planning, and smoke control system design in tunnel environments. Ultimately, this work demonstrates that rigorously validated CFD simulations can serve as practical alternatives to expensive and logistically complex full-scale fire testing. Building on these recent developments in BEV fire research and CFD validation practice, the present study provides a quantitative, multi-scenario validation of an HRR-driven FDS model against full-scale BEV and ICEV tunnel fire tests, with the aim of defining practical accuracy bounds for its use as an engineering tool.

## 2.0 EXPERIMENTAL TUNNEL BEV FIRE & CFD MODEL TEST SETUP

The tunnel fire tests conducted at Zentrum am Berg used sections of the road tunnels with a horseshoe-shaped cross section about 7.5 meters in height and 52 m<sup>2</sup> in area, similar to typical traffic tunnels [1]. The environment included realistic ventilation provided by jet fans with adjustable speeds to mimic real tunnel airflow and smoke control. Sensors for temperature, gas concentration, and velocity were strategically placed to capture spatial and vertical profiles of the fire and smoke dynamics shown in figure 1. These features make Zentrum am Berg an ideal controlled yet realistic setting for studying complex fire behaviors in tunnels, particularly those involving modern battery electric vehicles.

A series of full-scale five test vehicle (denoted as BV) fire tests were conducted in road tunnels to evaluate the fire behavior of BEVs under BV01 and BV05 compared to ICEVs of BV02, BV03 and BV04. Measurements included air temperature at multiple heights and locations, air velocity, HRR, and gas emissions such as toxic hydrogen fluoride from battery fires. Temperature measurements in the tunnel were obtained from type-K thermocouples arranged in vertical trees at several locations (hereafter referred to as thermocouples TC1.1–TC3.16). The tests revealed that BEV fires can exhibit higher peak heat release rates and prolonged burning due to battery involvement and thermal runaway events. The given dataset provides time-resolved temperature, air velocity, and HRR data from four distinct vehicle fire tests in the tunnel instead of five due to BV02 measurement data loss during the experiment. Hence, four case studies support further analysis and modelling, specifically for computational fluid dynamics (CFD) simulations in this paper.

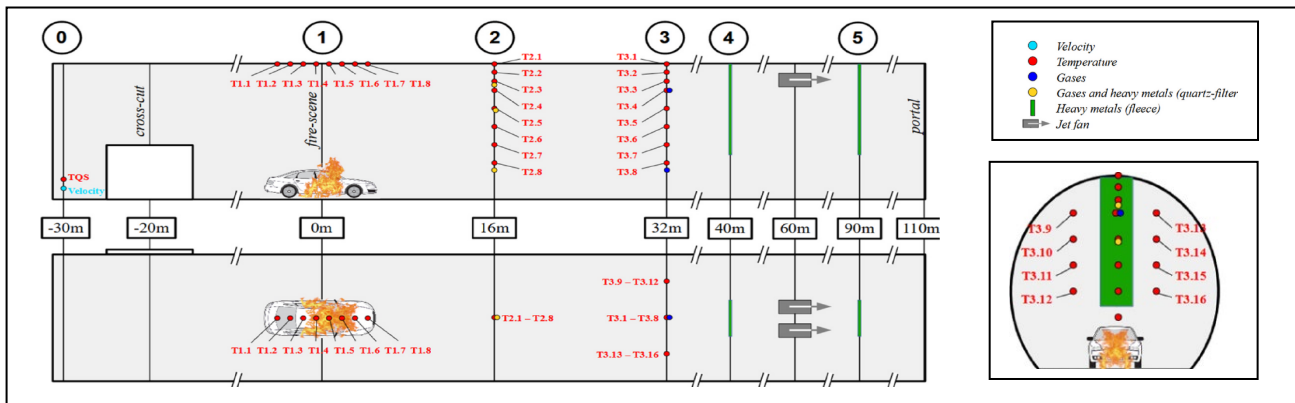
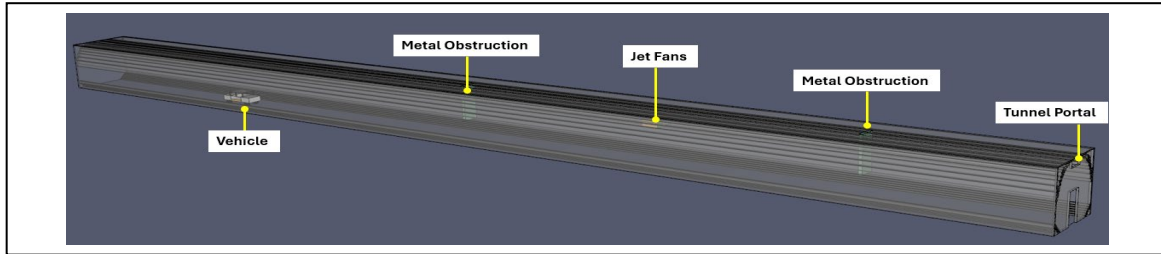


**Figure 1.** Schematic diagram of the full-scale tunnel fire test setup at Zentrum am Berg , showing vehicle position, thermocouple trees, and ventilation jet fans

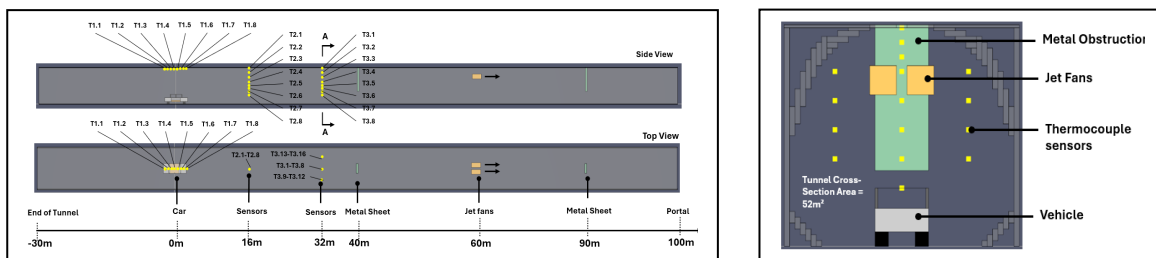
## 3.0 CFD SIMULATION & VALIDATION METHODOLOGY

The CFD simulation methodology for tunnel fire analysis employs the Fire Dynamics Simulator (FDS), which solves the Navier-Stokes equations for turbulent, low-Mach number flows with buoyancy effects, coupled with combustion and heat transfer modeling. Turbulence is represented using Large Eddy Simulation (LES) to capture transient turbulent structures critical to fire dynamics. Combustion is modeled based on mixture fraction and chemical reaction submodels, facilitating detailed representation of fuel burning and heat release consistent with experimental input [17]. Figure 2 shows the three-dimensional tunnel geometry replicates the physical setup of the "Zentrum am Berg" experimental facility, including tunnel dimensions, sensor locations, and environmental parameters, effectively creating a digital twin of the experiment. A key advantage of this approach is the direct use of experimentally measured time-dependent HRR as fire source inputs, isolating fluid dynamics and heat transfer predictions for validation.

Boundary conditions are specified to realistically simulate ambient temperature, humidity, pressure, and wall properties, while fire sources are applied as volumetric or surface heat sources based on measured HRR and fuel characteristics. The ventilation system, modeled through jet fans with prescribed flow rates, allows assessment of its effect on smoke movement and temperature distribution. This direct input of experimental HRR ensures the simulation replicates the exact energy release of the fire, thereby allowing temperature validation to focus specifically on the model’s accuracy in predicting fluid flow, heat transfer, and ventilation interaction.



(a)



(b)

**Figure 1.** Computational Fluid Dynamics (CFD) model setup: a) 3D geometry of the tunnel and vehicle, b) Location of Positioning of virtual thermocouples matching the experimental setup

Due to limitations in reproducing the exact geometry, fuel distribution and detailed battery pack configuration of the test vehicles, the fire source in the CFD model was idealised as a rectangular volume with dimensions  $2.0\text{ m} \times 2.0\text{ m} \times 0.5\text{ m}$ , representing the approximate footprint of the BEV battery pack or a generic fuel source region for ICEVs. This simplification allows the experimentally measured time-dependent HRR to be applied consistently while focusing the validation on the resulting flow and temperature fields rather than on detailed combustion and material decomposition processes. The validation focuses on comparing simulated and measured gas temperatures at multiple distances and heights, and does not include validation of smoke layer interface height, visibility, or toxic gas concentrations due to the lack of reliable experimental measurements for these quantities.

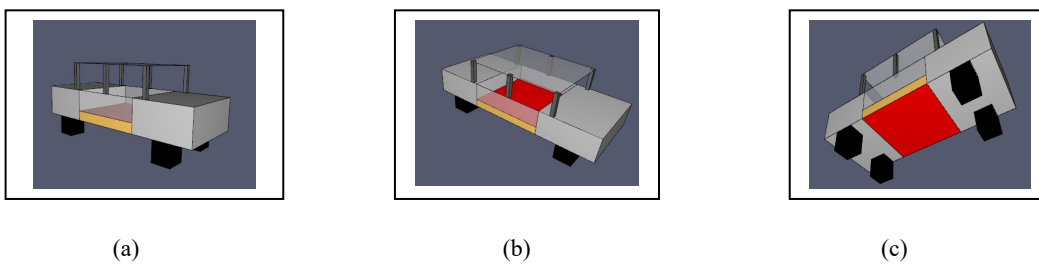


**Figure 2.** a) Test Vehicle used for analysis; b) Fuel source top location; c) Fuel source bottom location

### 3.1 Meshing Size and Resolution

The computational mesh (also referred to as the grid) discretises the tunnel and vehicle volume into finite cells for solving the governing equations, and in this paper the term “mesh” is used consistently to describe this discretisation. In tunnel fire modelling, the computational mesh covers both the tunnel volume and the vehicle so that the coupled fire and ventilation behaviour can be resolved.

The accuracy and efficiency of the simulation depend strongly on the chosen mesh cell size. To avoid complications from multiple mesh interfaces, a single uniform mesh is used in this study. A commonly used parameter

for selecting an appropriate mesh cell size, balancing accuracy and computational cost, is the characteristic fire diameter  $D^*$ , which is calculated using equation (1) :

$$D^* = \left( \frac{\dot{Q}}{\rho_{\infty} c_p T_{\infty} \sqrt{g}} \right)^{\frac{2}{5}} \tag{1}$$

Where

- $\dot{Q}$  indicates the  $HRR_{max}$  of the battery [in kW],
- $\rho_{\infty}$  represents the air density (1.204 kg/m<sup>3</sup>),
- $T_{\infty}$  indicates the ambient temperature (293.15 K),
- $c_p$  represents the specific heat capacity of the ambient air (1.005 kJ/kgK), and
- $g$  represents the acceleration due to gravity (9.81 m/s<sup>2</sup>).

In many practical cases,  $D^*$  is comparable to the physical diameter of the fire, and the corresponding non-dimensional heat release rate  $Q^*$  is of order 1. FDS uses Large Eddy Simulation (LES) to represent turbulent flow, with the unresolved “sub-grid” motion of the hot gases modelled by a sub-grid-scale turbulence model. The effectiveness of this approach depends strongly on the ratio of the fire’s characteristic diameter  $D^*$  to the grid cell size  $dx$ . The smaller the cell size, the finer the mesh; consequently, a larger ratio  $D^*/dx$  means that more of the fire dynamics are resolved directly and the simulation is generally more accurate. Previous studies and FDS guidance indicate that  $D^*/dx$  values between 5 and 10 usually provide favourable results at a moderate computational cost. As summarised in Table 1, the calculated ratios  $D^*/dx$ ,  $D^*/dy$  and  $D^*/dz$  for the considered HRR values fall within this range and were used to select a suitable mesh size for the model.

**Table 1.** Characteristic fire diameters of the analysed BV Vehicles Test No.

Test No.	HRR Max (kW)	D*	Ratio (D*/dx; D*/dy; D*/dz)					
			5	6	7	8	9	10
			Mesh Cell - dx; dy; dz					
BV01	7000	2.1	0.42	0.35	0.3	0.27	0.24	0.21
BV03	4900	1.9	0.38	0.32	0.28	0.24	0.22	0.19
BV04	2300	1.4	0.28	0.24	0.2	0.18	0.16	0.14
BV05	10000	2.3	0.46	0.39	0.33	0.29	0.26	0.23
Average Mesh Cell Size to be chosen			0.39	0.33	0.29	0.25	0.23	0.2

As shown in Table 1, the calculated ratios  $D^*/dx$ ,  $D^*/dy$  and  $D^*/dz$  lie between 5 and 10 for all vehicle fire scenarios. Based on these values, a uniform mesh cell size of 0.20 m was selected in the  $x$ ,  $y$  and  $z$  directions for all BV cases, corresponding to  $D^*/dx = 10$ , to provide good accuracy at a reasonable computational cost. Figure 4 illustrates the mesh arrangement, where selected boundary surfaces are defined as OPEN vents, representing interfaces to the external atmosphere outside the solid tunnel structure. With this configuration, the tunnel model comprises approximately 931,000 computational mesh cells

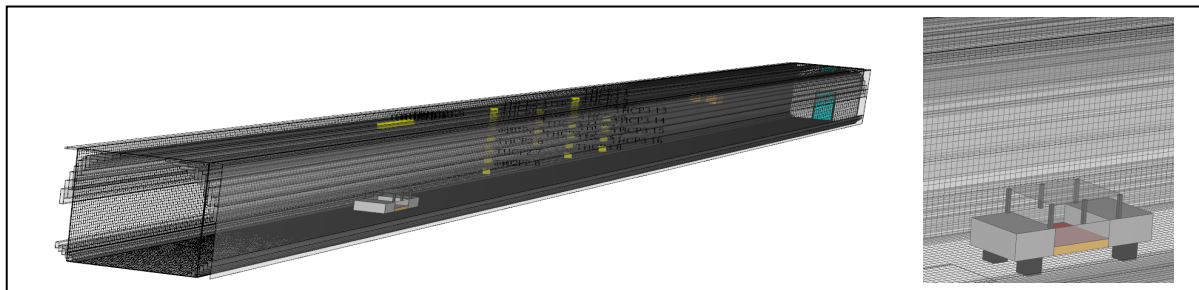


**Figure 3.** Mesh Grid Sizing 0.2m at dx, dy, dz highlighted in model analysis

### 3.2 Boundary and Initial Condition

The tunnel geometry is idealised, and uniform atmospheric conditions are assumed to reduce computational complexity and keep simulation times manageable. Minor features such as small protrusions, cable trays and surface roughness are neglected, and transient environmental effects (e.g. changing wind or ambient temperature) are not modelled. Where

experimental or site-specific data are unavailable, boundary conditions are inferred from the literature using uniform initial conditions and simplified ventilation profiles. Boundary conditions such as inlet air velocity, temperature and pressure are matched as closely as practicable to the experimental configuration, while acknowledging that some discrepancies remain due to these necessary simplifications.

For the CFD simulations, a set of pragmatic boundary and initial conditions is defined based on the local tunnel configuration and prior modelling experience. The experimentally measured HRR is used as the primary fire source input, as it directly quantifies the thermal energy release and governs the temperature distribution in the tunnel. Table 2 summarises the test vehicle characteristics, and Table 3 lists the environmental conditions, material properties and other parameters adopted as boundary and initial conditions.

Longitudinal ventilation is provided by jet fans mounted at the tunnel crown, consistent with the configuration used in the full-scale tests at Zentrum am Berg [1]. In the CFD model, each jet fan is represented as a velocity inlet aligned with the tunnel axis, generating an average longitudinal air velocity of approximately 2 m/s towards the traffic-flow portal. The jet fans operate continuously at this nominal speed for the duration of each scenario, giving a time-invariant ventilation profile representative of a quasi-steady longitudinal regime.

The tunnel portals are modelled as OPEN boundaries in FDS, allowing inflow and outflow of air and combustion products while maintaining the specified ambient pressure and temperature, as summarised in Table 3. All remaining solid surfaces, including the tunnel lining, road surface and vehicle body, are treated as thermally thick walls with thermophysical properties for concrete and steel taken from the literature. These choices capture the dominant heat transfer pathways without additional complexity from unresolved small-scale geometric details.

Turbulent motion of the hot gases and ventilation flow is resolved using Large Eddy Simulation (LES), with sub-grid-scale turbulence represented by the standard FDS model. Turbulence arises from the resolved shear layers at the jet fan outlets, the fire plume and interaction with the tunnel walls; no explicit turbulence intensity or synthetic turbulence is prescribed at the inlets, consistent with common practice for longitudinally ventilated tunnel simulations [17]. Combined with the experimentally measured, time-dependent HRR applied as a volumetric source, these boundary conditions define a reproducible CFD setup that captures the main features of the experimental tunnel fire environment.

**Table 2.** Test BV vehicle relationship used in Model Analysis

Test No.	Vehicle (Model Year)	Battery/Fuel Capacity	HRR max (kW)	Fire Duration time (seconds)	Note
BV01	Compact (Car 2020)-BEV1	80 kwh	7000	1050	Battery failure mode gradually by few cells & Fire Blanket Extinguishment after 500s
BV03	ICEV3, SUV (2020)	Unknown, Diesel	4900	2400	Exact amount of fuel unknown
BV04	ICEV4, Van (2010)	50 Liter Diesel	2300	1800	Utility van loading space totally empty
BV05	SUV (2020)-BEV 5	80 kwh	8600	1750	Battery Thermal runaway after 10min (Car & Battery)

\*Measurement experiment data failure excluded from the validation process

**Table 3.** Boundary condition setting parameters for the analysis

Environment Condition [1]	
Ambient air temperature	11°C
Ambient pressure	101325 Pa
Relative air humidity	80%
Wind speed	0 m/s
Tunnel Boundary Condition (Concrete) [10]	
Density	2280 kg/m <sup>3</sup>
Thermal conductivity	1.8 W/mK
Specific heat	1.04 kJ/kgK
Emissivity	0.9
Car Vehicle Boundary Condition and Other Metal Obstruction [11]	
Density	7850 kg/m <sup>3</sup>
Thermal conductivity	45.8 W/mK
Specific heat	0.46 kJ/kgK
EV vehicle car dimension	5000mm (L) x 2000mm (W) x 1500mm (H) [12]
Battery/ Fuel Source fire scenario	2000mm (L) x 2000mm (W) x 500mm (H)
Combustible Material Upholstery (Polyurethane) [13]	

Chemical Formula (C <sub>1</sub> H <sub>1.7</sub> O <sub>0.3</sub> N <sub>0.08</sub> )	C (Carbon atom -1) H (Hydrogen atoms -1.7) O (Oxygen atoms -0.3) N (Nitrogen atoms -0.08)
Soot Yield	0.1 kg/kg
Carbon Monoxide (CO) Yield	0.042 kg/kg
Heat of combustion	31,000 kJ/kg [15]
<b>Thermocouple (TC) Parameter [14]</b>	
Bead Diameter	0.33mm
Emissivity	0.2
Bead Density	8908.0 kg/m <sup>3</sup>
Bead Specific Heat	0.44 kJ/kgK)
<b>Jet Fan Profile [1]</b>	
Jet Fan Flow Capacity	2 m/s
Speed	Constant
Air Flow Condition	Quasi-Steady State
<b>Computational Meshing Grid Dimension</b>	
X, Y, & Z directions	0.2m x 0.2m x0.2m
Total Mesh Sizing	931,000

### 3.3 Root Mean Square Error (RMSE) Validation

After the CFD model was run, the results were evaluated using Root Mean Square Error (RMSE) approach due to is common, powerful, and highly recommended for specific purposes in any CFD validation papers. It provides a single, quantitative measure to assess the agreement between CFD results and experimental data. The RMSE was calculated to quantitatively assess the discrepancy between the experimental and Computational Fluid Dynamics (CFD) temperature datasets by this following equation (2).

$$RMSE = \sqrt{\frac{\sum_{i=1}^N \|y(i) - \hat{y}(i)\|^2}{N}} \quad (2)$$

$\Sigma$  is the summation

$y_i$  is the actual value at data point  $i$

$\hat{y}_i$  is the predicted value at data point  $i$

$N$  is the total number of data points.

This statistical metric provides a single value, expressed in degrees Celsius, which represents the standard deviation of the residuals which is the differences between the measured experimental data and the CFD-predicted values. A non-zero RMSE confirms that deviations exist, and its magnitude directly indicates the average magnitude of these prediction errors across all measured points and times during the fire events.

## 4.0 RESULTS AND DISCUSSION

The CFD model demonstrates strong qualitative agreement with the experimental HRR data for all vehicle fire scenarios, both BEV and ICEVs, as shown in Figure 5. The alignment of CFD predicted HRR trends with experimental measurements highlights the model's ability to accurately incorporate dynamic fire source inputs. This fidelity in HRR input is foundational for reliable temperature prediction downstream in the tunnel environment. The temperature trend comparisons across distances 0 m, 16 m, and 32 m (Figures 6-9) show the CFD model captures key thermal behaviors in these fires. Specifically, the model reproduces the general shape, peak, and decay phases of the temperature curves, indicating its competency in simulating transient fire dynamics.

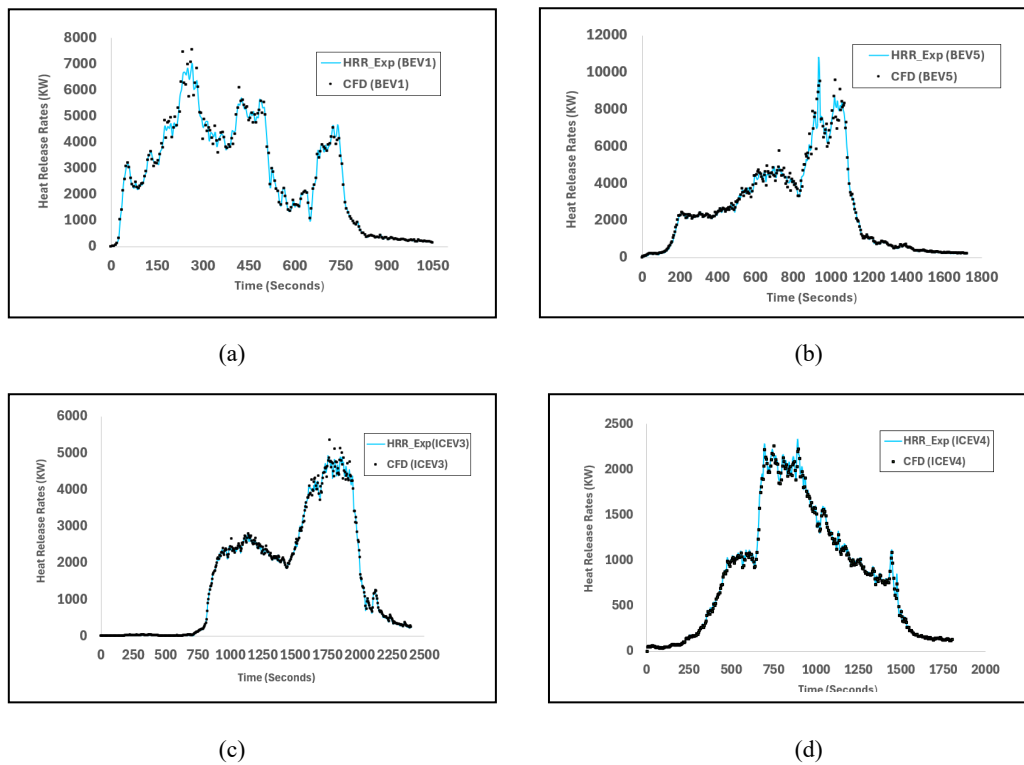
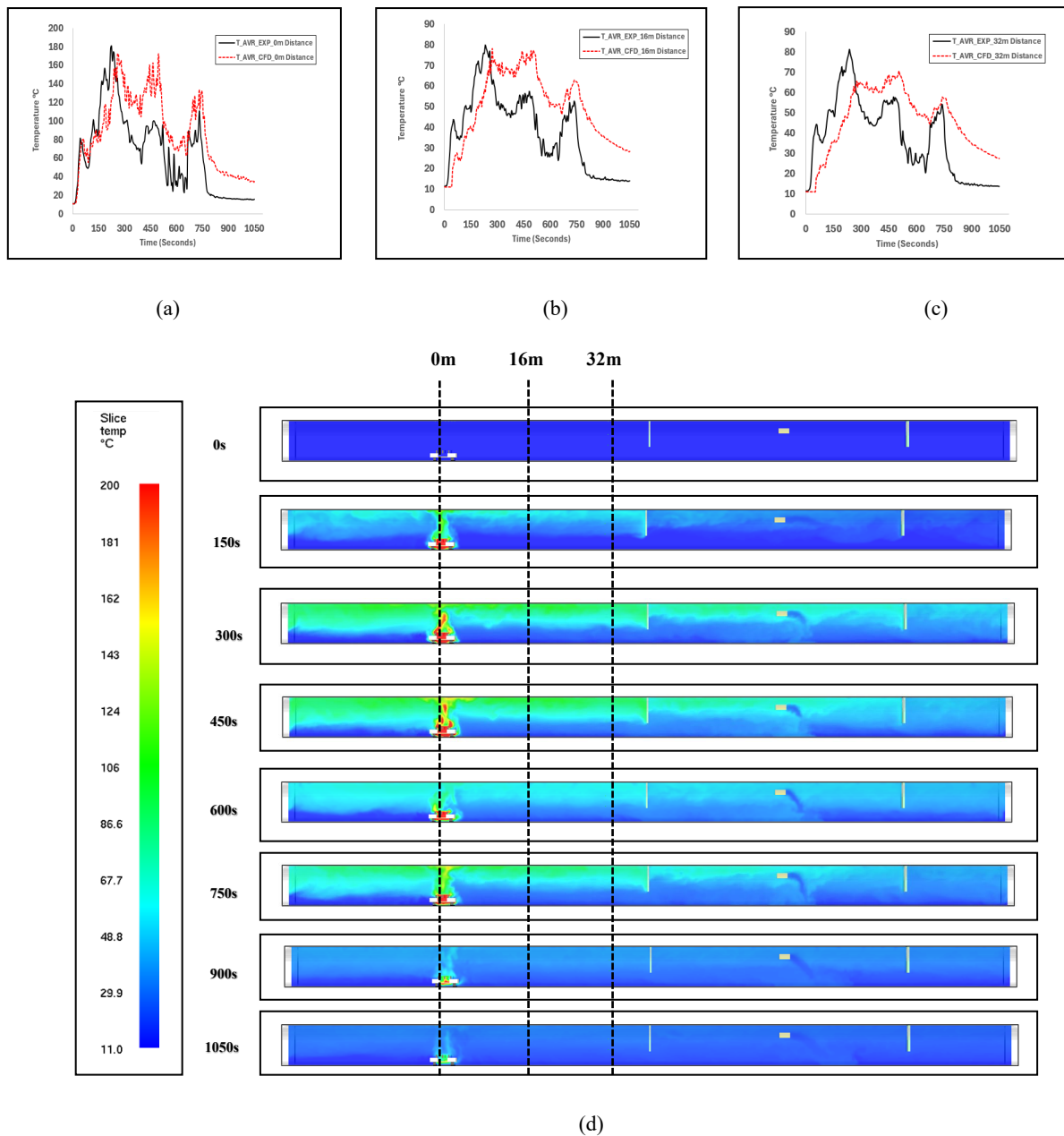


**Figure 4** : Comparison between CFD output and experiment HRR vehicle fire scenarios; a) BV01; b) BV05; c) BV03; & d) BV04

For simplicity, the average temperature readings were calculated at three defined distance intervals within the tunnel: 0 m (averaging readings from thermocouples TC1.1 to TC1.8), 16 m (thermocouples TC2.1 to TC2.8), and 32 m (thermocouples TC3.1 to TC3.16). These averaged values effectively summarize the overall temperature distribution at each interval and are used to compare against the CFD simulation results, as shown in Figures 6 to 9. Additionally, temperature profile snapshots from the CFD model at different tunnel sections were extracted to provide further insight into the temperature variations within the tunnel environment.

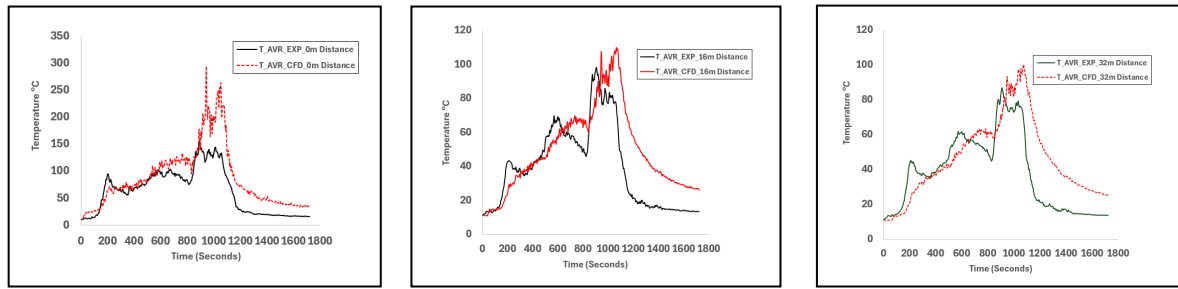
#### 4.1 Overview of CFD Graph Validation Findings

Figure 6 presents a comparison of temperatures between experimental data and CFD predictions for the BV01 BEV fire test, measured at distances of 0 m, 16 m, and 32 m from the fire source. This test uniquely involved igniting the BEV battery by directly injecting a saline solution (NaCl<sub>aq</sub>) into the battery pack, which induced an internal short circuit and triggered the fire. Where a BEV fire starts from the battery, but only from a few cells, then a slower onset thermal runaway event characterized by gradual battery cell failure and sustained heat release around 7 MW [1]. The CFD model closely follows the experimental temperature trends, accurately capturing the fire's rise, peak, and decay phases, especially at distances of 16 m and 32 m from the fire source. Slight discrepancies near the fire origin (0 m) are observed due to the complex transient thermal runaway processes and the application of a fire blanket at 500 seconds, which complicate precise modeling. Overall, the CFD simulation demonstrates strong capability in representing the sustained BEV fire behavior, which is characterized by gradual heat buildup rather than rapid, explosive events.

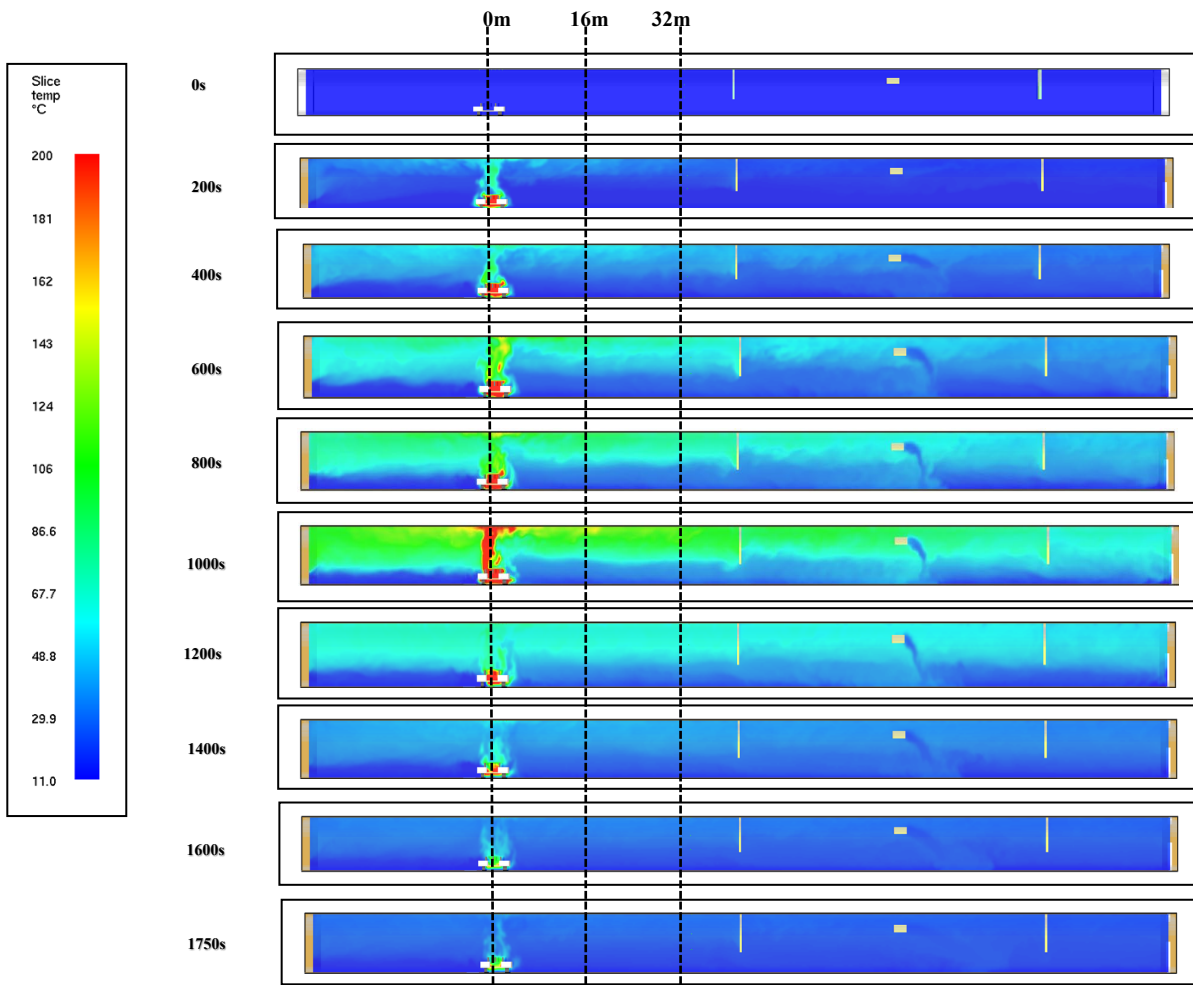


**Figure 5.** BV 01 Average Experiment Temperatures versus average CFD Temperatures; a) 0m Distance, b) 16m Distance, & c) 32m Distance d) Snap shots CFD temperature profile at Y direction centre of the ignition vehicle fire source.

On the other hand, the CFD trendlines in Figure 7 effectively capture the sharp, high peak HRR caused by rapid, simultaneous failure of battery cells in the BV05 fire scenario (BEV), reaching approximately to 10 MW. The experimental data indicates after 10 minutes, a sudden onset of thermal runaway, driven by internal short circuits and chemical decomposition within the battery, which results in intense exothermic reactions releasing both heat and flammable gases. The CFD predictions closely follow this behavior, especially at the 16 m and 32 m distances, accurately representing the rapid temperature fluctuations and peak HRR. Greater discrepancies near 0 m again highlight the challenge of modelling fast transient events and fire source dynamics. Although minor discrepancies are observed near the fire source at 0 m, likely due to the extreme transient dynamics and variability in the heat release peaks, overall, the model demonstrates a strong transient response. This confirms again that the CFD approach successfully simulates the rapid escalation characteristic of a BEV thermal runaway event, including the violent and sudden increase in heat flux, making it a reliable tool for analyzing high-intensity fire scenarios involving electric vehicles with fast cell failure mechanisms.



(a) (b) (c)



(d)

**Figure 6 :**BV 05 Average Experiment Temperatures versus average CFD Temperatures; a) 0m Distance, b) 16m Distance, & c) 32m Distance, d) Snap shots CFD temperature profile at Y direction centre of the ignition vehicle fire source.

Figure 8 compares temperature results from the BV03 is an ICEV fire test. The ICEV fire is of lower intensity, generally at 4.9 MW heat release, and displays relatively stable combustion behavior of liquid fuel. The CFD and experimental temperature trends match closely at all measured distances, accurately representing the growth, peak, and cooling phases typical of ICEV fires. The simpler and more predictable combustion characteristics of ICEV fires contribute to the tighter agreement between measured and predicted temperatures. This result supports the reliability of the CFD model for conventional vehicle fire simulations where combustion dynamics are less complex than in BEVs. The predictability and lower intensity of ICEV fires compared to battery electric vehicle fires make CFD modeling more straightforward and yield a tighter correlation with experimental results. This validation supports the use of the CFD approach as a reliable tool for assessing fire safety and risk in tunnels involving conventional vehicle fire scenarios, where combustion

progresses steadily without the transient complexities seen in thermal runaway events common to BEVs

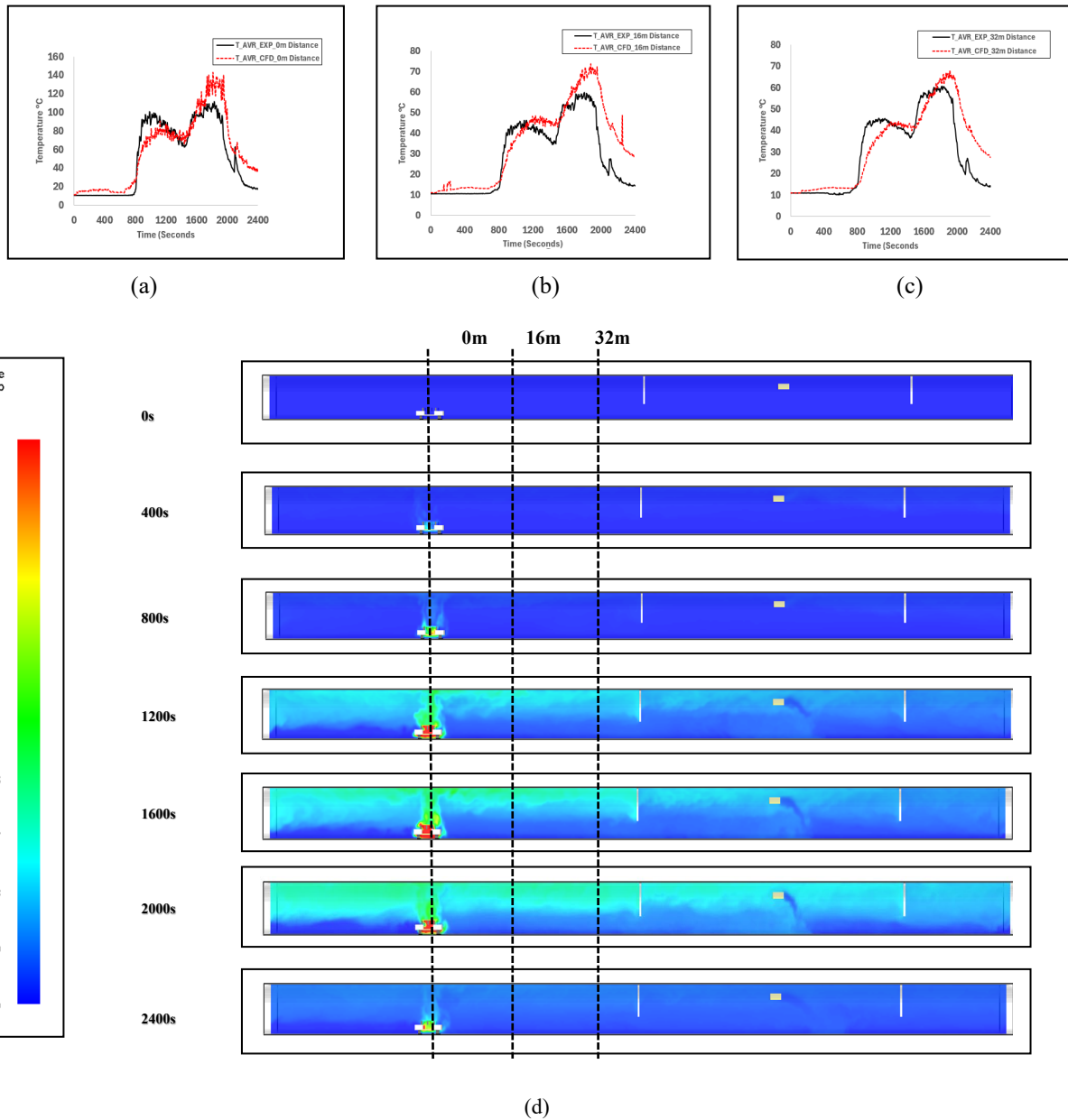
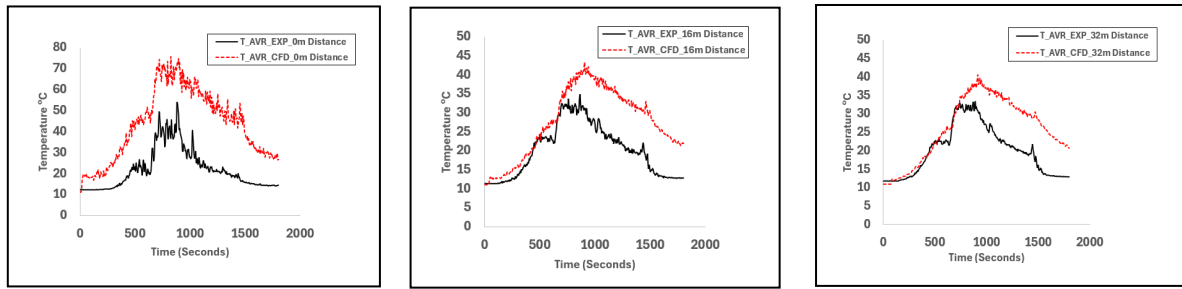
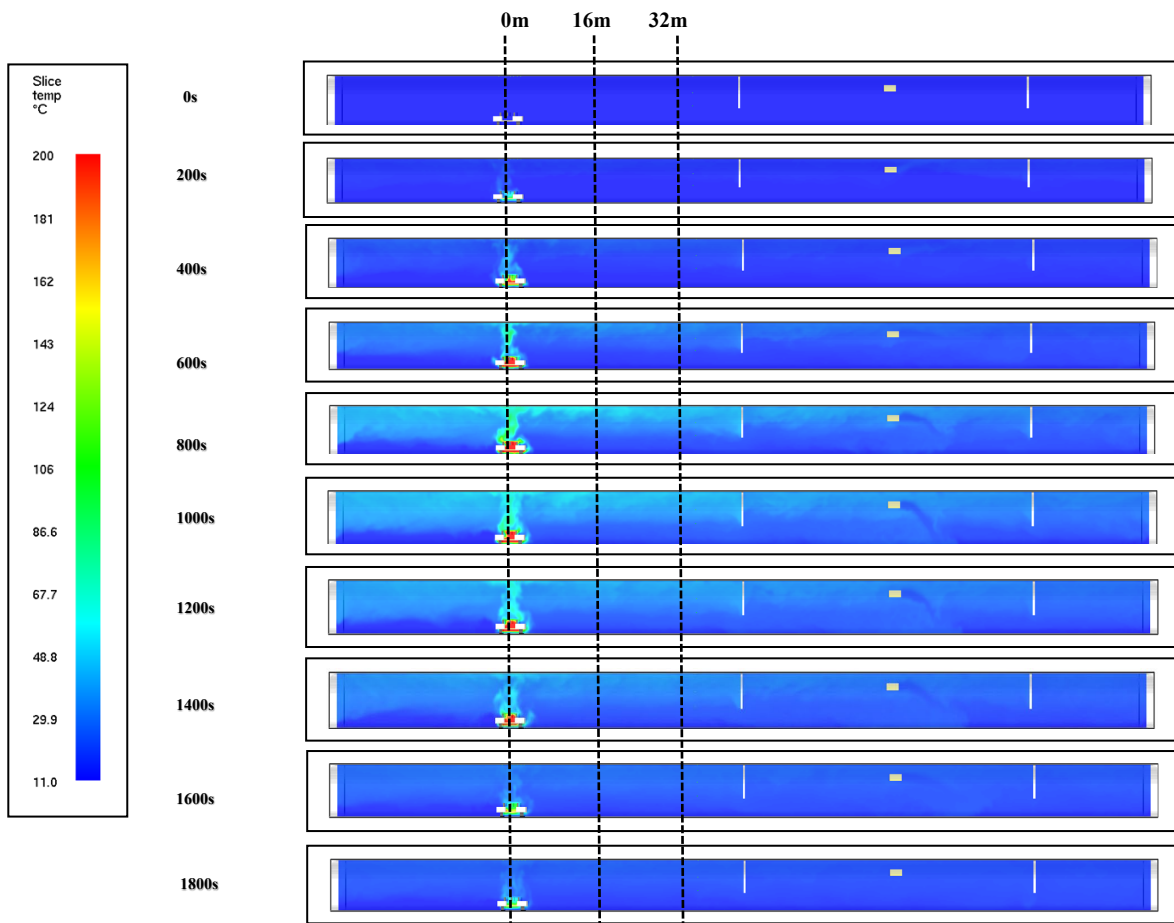


**Figure 7.** BV 03 Average Experiment Temperatures versus average CFD Temperatures; a) 0m Distance, b) 16m Distance, & c) 32m Distance, d) Snap shots CFD temperature profile at Y direction centre of the ignition vehicle fire source.

Figure 9 another presents the BV04 ICEV fire test, showing steady combustion behavior with clearly defined peak and decay temperature phases at 2.3 MW much lower HRR. The CFD temperature curves closely overlap the measured experimental data at distances of 0 m, 16 m, and 32 m, indicating a high degree of accuracy in the simulation. The finding provides another strong agreement between CFD, and experiment validates the model's capability to capture the fire dynamics typical of ICEV scenarios, supporting its practical application in fire safety design and risk assessment for tunnels exposed to conventional vehicle fires



(a) (b) (c)



(d)

**Figure 9.** BV 04 Average Experiment Temperatures versus average CFD Temperatures; a) 0m Distance, b) 16m Distance, &c) 32m Distance, d) Snap shots CFD temperature profile at Y direction centre of the ignition vehicle fire source.

Together, these figures illustrate how the CFD model effectively captures temperature evolution for both BEV and ICEV fires at multiple spatial points downstream of the fire source, with increasing accuracy at greater distances due to plume stabilization and heat dissipation. Challenges remain in modeling rapid transient phenomena and localized combustion near the fire origin, especially for BEVs, which produces higher error margins. Nonetheless, the CFD model's capacity to reproduce the main thermal features across different fire types strengthens its utility as a predictive tool for tunnel vehicle fire analysis.

#### 4.2 Quantitative Accuracy of RMSE and Percentage Error

The CFD model shows strong qualitative and quantitative agreement with the experimental temperature data over time and at different measurement locations for both BEV and ICEV fire tests. The main deviations occur near the fire source

and during rapid transient phases typical of BEV battery thermal runaway, underlining the inherent difficulty of modelling complex electrochemical fire dynamics. To quantify model accuracy, the RMSE metric was applied to measure the average deviation between CFD predictions and experimental thermocouple readings across all fire scenarios. The detailed thermocouple-wise RMSE values for each test and distance are provided in Appendix A (Table A1), while Table 4 summarises the average RMSE and percentage error at 0 m, 16 m and 32 m for each vehicle fire test. These values provide overall error measures averaged over multiple sensors and time points, and therefore characterise the representative accuracy of the CFD model for each scenario.

RMSE measures the average magnitude of the differences between predicted CFD and observed (experimental) values, expressed in the same units as temperature. A lower RMSE indicates a closer fit of the CFD results to experimental data and thus greater predictive accuracy, whereas higher RMSE values indicate larger discrepancies. To place these values in context, the average percentage error is evaluated relative to a representative experimental temperature at each location, taken as the maximum experimental temperature ( $T_{max\_exp}$ ). This links the error directly to the intensity and thermal severity of each fire scenario. The percentage error is computed using equation (3), and the resulting averages for all cases and distances are reported in Table 4.

$$\frac{\text{Average RMSE at distance}}{\text{Average } T_{max\_exp} \text{ at distance}} * 100\% = \text{Average Percentage Error (\%)} \text{ at distance} \tag{3}$$

**Table 4** : Average Percentage Error for Each Test No at 0, 16 & 32m distance

Test No.	Vehicle Type	Distance (m)	Average RMSE (°C)	Average Temperature max (°C)	Average Percentage Error (%)
BV01	BEV	0	37.3	185.3	20.1
		16	20.3	83.8	25.1
		32	21.3	85.8	25.4
BV03	ICEV	0	13.4	114	11.7
		16	6.1	63	9.7
		32	7.4	63	11.9
BV04	ICEV	0	24.3	60	40.0
		16	9.0	35	25.7
		32	8.3	35	24.6
BV05	BEV	0	38.8	157	26.2
		16	20.1	101	21.3
		32	20.7	89	25.2

Table 4 highlights several critical aspects of the CFD model’s validation against experimental tunnel fire data. The average percentage error generally decreases with increasing distance from the fire source, with the highest errors near the source (0 m), reflecting the inherent complexity and localised heat release phenomena that are more difficult to model accurately. At greater distances (16 m and 32 m), the fire plume becomes more stable, leading to reduced errors and improved replication of the measured thermal gradients. BEV fire tests consistently show higher percentage errors (approximately 20–26%) compared with ICEV tests (approximately 10–15%), which is attributed to the more complex combustion dynamics of lithium-ion battery fires that are not fully captured by the simplified combustion model.

Despite these discrepancies, the error magnitudes mostly fall within widely accepted engineering tolerances of about 10–30% for fire CFD modelling in tunnels [9], where exact numerical correspondence is limited by turbulent, buoyancy-driven flow processes and experimental uncertainties. The consistency of the error levels across different tests and sensor locations underscores the robustness and repeatability of the CFD methodology, enabling a reliable assessment of simulation accuracy relative to experimental benchmarks. Overall, Table 4 effectively conveys both the strengths of the validated CFD model in capturing key thermal behaviours and its limitations related to fire source complexity and modelling assumptions, supporting its use as a reliable and cost-effective tool to complement physical fire testing in tunnel fire safety engineering.

The CFD model shows strong qualitative and quantitative agreement with the experimental temperature data over time and at different measurement locations for both BEV and ICEV fire tests. The main deviations occur near the fire source and during rapid transient phases typical of BEV battery thermal runaway, underlining the inherent difficulty of modelling complex electrochemical fire dynamics. To quantify model accuracy, the RMSE metric was applied to measure the average deviation between CFD predictions and experimental thermocouple readings across all fire scenarios. The detailed thermocouple-wise RMSE values for each test and distance are provided in Appendix A (Table A1), while Table 4 summarises the average RMSE and percentage error at 0 m, 16 m and 32 m for each vehicle fire test. These values provide overall error measures averaged over multiple sensors and time points and therefore characterise the representative accuracy of the CFD model for each scenario.

### **4.3 Interpretation of Model Performance and Utility**

The observed discrepancies, notably the consistent approximate 20–26% error in the far field for BEV fires, do not undermine the validity of the model; instead, they define its practical performance boundaries. This trend suggests a systematic difference, likely related to plume radiation or entrainment processes specific to battery fires, that is not fully represented by the simplified combustion model. Recognising this discrepancy is an important outcome of the validation exercise, as it quantifies where and by how much the model departs from the experimental behaviour.

For engineering applications, these error levels are acceptable. Fire safety design inherently incorporates factors of safety, so a model that reliably captures the dominant trends and remains within a reasonable error margin is highly valuable. In this context, the validated model can be used with confidence for future fire simulation analyses, helping to supplement or reduce the need for costly full-scale fire tests. The comparison between experimental and CFD temperature datasets across all tunnel EV fire tests therefore provides not only a measure of model accuracy but also clear insight into its limitations, as discussed in the following sections

#### **4.3.1 Fire Source Representation**

Elevated RMSE values near the fire source, especially at sensors located at 0 meters, primarily result from simplified fire source modeling. Although the CFD simulations use measured heat release rate (HRR) data to represent fire size, they do not incorporate detailed combustion chemistry or the complex fuel characteristics inherent in lithium-ion battery or hydrocarbon fires. This simplification compromises the accuracy of localized temperature predictions where fire dynamics and material interactions are most complex.

#### **4.3.2 Boundary Condition Assumptions**

Boundary conditions in the CFD models are based on the available experimental data, which carry inherent limitations. Simplifications and assumptions were required to make the simulations computationally feasible, but these contribute to deviations between predicted and measured results. Specifically, modeling transient ventilation effects and tunnel airflow dynamics accurately remains challenging due to their complex and variable nature.

#### **4.3.3 Time-Dependent Factors**

CFD-predicted temperature response curves generally align well with experimental data in the time window of approximately 200 to 500 seconds. Beyond this period, discrepancies tend to increase, attributed to the growth of turbulence and ventilation-induced fluctuations in the fire environment, which complicate model stability and predictive precision. Such temporal variations are common in tunnel fire simulations and underscore the intricacies in capturing long-duration, complex fluid dynamics.

#### **4.3.4 Material Assumptions**

Due to limitations in the available real-world data for type K thermocouples, the CFD model relies on general thermocouple data rather than specific experimental measurements. Additionally, the model employs simplified material properties, using generic plastic characteristics for vehicle components instead of detailed, accurate representations of the actual materials involved. Since actual vehicle fires involve heterogeneous materials with varying thermal properties, incorporating more detailed material models could improve accuracy and potentially lower RMSE values by better capturing heat release dynamics. Despite these acknowledged limitations, the CFD predictions successfully replicate the qualitative temperature trends observed in the experimental data, with RMSE values around 20%. This level of agreement is consistent with accepted validation standards for fire CFD modeling. The strong correlation between CFD trendlines and experimental measurements indicates that the current model settings and assumptions are adequate for capturing the essential thermal behavior of tunnel fires involving BEV battery fires. Nonetheless, further improvements in model accuracy are possible by obtaining more detailed input data and refining boundary condition inputs

#### **4.3.5 Scope and limits of applicability**

Overall, the validation results indicate that the present FDS model can reproduce the main temporal and spatial temperature trends for full-scale BEV and ICEV tunnel fires within average error ranges of about 10–15% for ICEV tests and 20–26% for BEV tests at distances beyond 16 m from the fire source. These values, together with the discussed sensitivities to fire source idealisation, boundary conditions, material properties and long-duration turbulence effects, define the practical performance envelope of the model. Within this envelope, the model is suitable for engineering analyses such as parametric studies, ventilation strategy assessments and preliminary risk evaluations, but it should not be interpreted as a fully predictive tool for arbitrary tunnel geometries, ventilation regimes or alternative vehicle and battery configurations without additional case-specific validation

#### 4.4 Summary

The CFD model demonstrated strong capability in validating the experimental temperature data across all tested scenarios, including BV01, BV03, BV04, and BV05. The validation is supported by three key findings. First, the simulations accurately captured the transient characteristics of the fires, encompassing the growth phase, peak intensity, and decay period. The close alignment of the model's output with the experimental temperature curves confirms its ability to simulate the dynamic progression of the fire over time. Second, the model successfully predicted the spatial temperature gradients, demonstrating the expected decrease in temperature as the distance from the fire source increased. This consistency with experimental measurements validates the model's representation of fundamental fire physics such as plume rise and heat dissipation. Third, quantitative analysis using RMSE coupled with percentage error calculations showed that the model achieved high accuracy approximately 11% error for the ICEV test (BV03) and somewhat higher but still consistent and quantifiable errors between 20% and 26% for the more complex BEV fire tests (BV01, BV05). These conclusions apply to the specific tunnel geometry, ventilation conditions and vehicle fire scenarios considered in this study, and further validation would be required before extrapolating the model directly to different tunnel layouts, ventilation strategies or battery technologies

The discussion highlights model limitations such as simplified fire source representation, boundary condition assumptions, time-dependent turbulence effects, and generic material property use, which influence prediction accuracy. Despite these constraints, the model's results fall within generally accepted engineering tolerance levels for fire CFD modeling, making it a valid and valuable tool for supplementing physical fire testing. Table 4 provides a systematic comparison of average percentage errors across distances and vehicle types, showing consistent and interpretable performance trends. This quantitative validation supports the CFD model's reliability and applicability for future tunnel fire safety analysis, offering a cost-effective, flexible alternative to full-scale experimental testing. Overall, Chapter 4 justifies the model's use as a robust "digital twin" that enhances understanding of vehicle fire behavior in tunnels and supports fire safety engineering decisions. This substantiates that the model is not only qualitatively reliable, capturing key thermal trends, but also quantitatively robust enough to be used confidently for engineering and fire safety design purposes.

#### 5.0 CONCLUSION

The study successfully validates a CFD model against experimental full-scale tunnel fire tests involving both BEVs and ICEVs. The model, using measured HRR data as direct input, reliably replicates temperature distributions and fire dynamics within acceptable engineering accuracy, as evidenced by RMSE and percentage error analyses. This validation demonstrates the CFD model's capability as a robust "digital twin" of physical experiments, capturing essential thermal behaviors, spatial gradients, and temporal fire development. While inherent simplifications such as idealized combustion chemistry, boundary assumptions, and generic material properties necessitate cautious interpretation, the model's performance falls well within industry-accepted tolerance levels. Consequently, the validated CFD approach provides a cost-effective, flexible, and practical tool that complements traditional fire testing. It supports detailed fire safety design, risk assessment, and emergency planning for tunnel environments with emerging BEV fire hazards, reducing dependence on costly and logistically complex physical experiments. While acknowledging some limitations stemming from model simplifications and assumptions, the consistency across multiple scenarios affirms the CFD model's practical applicability for tunnel fire safety analysis. Future work should focus on refining combustion and material modeling, incorporating more detailed chemical kinetics, and improving transient boundary conditions to further enhance predictive accuracy. Nonetheless, this study establishes a strong foundation for employing CFD simulations to inform fire safety engineering decisions sustainably and effectively.

#### ACKNOWLEDGMENTS

The authors would like to express their appreciation information of this project was funded by the Austrian Government, BMK (former BMVIT) and ASFINAG. Special thanks also to Andrea Schirmer, Thomas Nöst, Philip Leonhardt and Alexander Hödl (all Graz University of Technology) as well as to Bernhard Reinwald (Montanuniversität Leoben) for their valuable data information and the Faculty of Chemical Engineering, University Putra Malaysia (UPM).

#### REFERENCES

- [1] Sturm P, Föbleitner P, Fruhwirt D, Galler R, Wenighofer R, Heindl SF, Krausbar S, Heger O. Fire tests with lithium-ion battery electric vehicles in road tunnels. *Fire Safety Journal*. 2023;134:103695.
- [2] Sturm P, Föbleitner P, Fruhwirt D, Heindl SF, Heger O, Galler R, Wenighofer R, Krausbar S. Dataset of fire tests with lithium-ion battery electric vehicles in road tunnels. *Data in Brief*. 2023;46:108839.
- [3] Kashaf A, Saber HH. Application of CFD techniques for modelling fire tests in road tunnels. In: 5th International Conference on Tunnel Safety and Ventilation; 2010; Graz, Austria. p. 221–228. (Ville-Marie Tunnel, Tube C ventilation verification).

[4] Woodburn P, Britter RE. CFD simulations of a tunnel fire—Part I. Fire Safety Journal. 1996;26(1):35–62. doi:10.1016/03797112(96)00018-5.

[5] Woodburn P, Britter RE. CFD simulations of a tunnel fire—Part II. Fire Safety Journal. 1996;26(1):63–90. doi:10.1016/0379-7112(96)00019-7.

[6] BRAFA. Fire effects of vehicles with alternative drive systems (BRAFA). Project entry, Austrian Research Promotion Agency (FFG); accessed 5 May 2022. Available from: <https://projekte.ffg.at/projekte/3290205>.

[7] Föbtleitner P, Sturm P. “BRAFA” – project, measurement data. Data repository, Graz University of Technology; 2021. doi:10.3217/ysgwn-3a318.

[8] Vidmar P. Risk evaluation in road tunnels based on CFD results. Thermal Science. 2022;26(2B):1432–1450. doi:10.2298/TSCI201108174V.

[9] Reszka P, Steinhaus T, Biteau H, Carvel R, Rein G, Torero JL. Study of fire durability for a road tunnel: Comparing CFD and simple analytical model. In: 4th International Conference on Tunnel Safety and Ventilation; 2008; Graz, Austria. p. 163–172.

[10] Krishnamoorthy RR, Saleheen Z. Numerical simulation of spalling and moisture evaporation in concrete tunnel linings exposed to fire. In: Kodur V, Agrawal A, editors. Fire performance of high-strength concrete structures. Singapore: Springer; 2022. p. 801–818. doi:10.1007/978-981-16-7924-7\_57.

[11] Singh R. Lightweight metals and alloys in electric vehicle manufacturing: Enhancing performance and efficiency. International Journal of Scientific Research and Applications. 2024;13(2):143–152. doi:10.30574/ijrsra.2024.13.2.2343.

[12] Ministry of Housing and Local Government (KPKT). Planning Guidelines for Electric Vehicle Charging Bay (EVCB). 1st ed. Putrajaya (Malaysia): KPKT; 2023.

[13] Rosenbaum ER, editor. SFPE Engineering Guide to Performance-Based Fire Protection. 2nd ed. Quincy (MA): Society of Fire Protection Engineers and National Fire Protection Association; 2007.

[14] Lecocq A, Bertana M, Truchot B, Marlair G. Comparison of the fire consequences of an electric vehicle and an internal combustion engine vehicle. In: 2nd International Conference on Fires in Vehicles (FIVE 2012); 2012; Chicago, IL, USA.

[15] Forney GP. User’s Guide for Smokeview Version 5 – A tool for visualizing Fire Dynamics Simulation data. NIST Special Publication 1017-1. Gaithersburg (MD): National Institute of Standards and Technology; 2007. 134 p.

[16] McGrattan K, Hostikka S, Floyd J, Baum H, Rehm R, Mell W, et al. Fire Dynamics Simulator (Version 5): Technical Reference Guide, Volume 1 – Mathematical model. NIST Special Publication 1018-5. Gaithersburg (MD): National Institute of Standards and Technology; 2009. 94 p.

[17] McDermott RJ, Forney GP, McGrattan K, Mell WE. Fire Dynamics Simulator Version 6: Complex geometry, embedded meshes and quality. NIST Technical Note 1889. Gaithersburg (MD): National Institute of Standards and Technology; 2015.

[18] McDermott RJ, Forney GP, McGrattan K, Mell WE. Fire Dynamics Simulator Version 6: Complex geometry, embedded meshes, and quality assessment. National Institute of Standards and Technology; June 2010.

[19] Sturm, J., Oplustil, J., Fasser, M., and Biegl, J., “Fire tests with lithium-ion battery electric vehicles in road tunnels,” *Tunnelling and Underground Space Technology*, 125, 104528, 2022.

[20] Kohl, A., Rattei, G., Sturm, J., and Fasser, M., “Investigation of fires with electric vehicles in underground traffic areas,” *Tunnel*, 2021

[21] Sturk, D., Ekelund, M., and Blomqvist, P., “Analysis of combustion gases from large-scale electric vehicle battery fires,” *Fire Safety Journal*, 141, 103021, 2023.

[22] Larsson, F., Andersson, P., and Mellander, B.-E., “A review of battery fires in electric vehicles,” RISE report, 2020.

[23] Moser, A., “CFD simulation validation for tunnel ventilation – a case study from the Arlberg Tunnel,” University of Leoben, 2025.

[24] Papapostolou, K. et al., “Smoke extraction in a sinusoidal floor tunnel: experimental and numerical study,” *Emerging Materials and Structural Technology*, c. 2022–2023.

**APPENDIX**

**Table A1.** RMSE obtained value based on every thermocouple (TC) temperature location

Root Mean Square Error (°C) Value at distance Interval for 0m, 16m and 32m												
TC	Test No: BV 01			Test No: BV 03			Test No: BV 04			Test No: BV 05		
	0m	16m	32m	0m	16m	32m	0m	16m	32m	0m	16m	32m
1.1	29.8	-	-	16.2	-	-	20.8	-	-	24.4	-	-
1.2	39.5	-	-	18.6	-	-	27.6	-	-	33.9	-	-
1.3	37.3	-	-	15.0	-	-	27.1	-	-	37.3	-	-
1.4	39.5	-	-	12.7	-	-	29.6	-	-	40.2	-	-
1.5	38.7	-	-	10.8	-	-	26.2	-	-	43.2	-	-
1.6	38.4	-	-	11.0	-	-	23.9	-	-	44.4	-	-
1.7	38.3	-	-	11.3	-	-	21.6	-	-	44.0	-	-
1.8	36.8	-	-	11.5	-	-	18.0	-	-	42.9	-	-
2.1	-	23.8	-	-	6.59	-	-	10.3	-	-	25.3	-
2.2	-	24.9	-	-	8.19	-	-	11.6	-	-	25.1	-
2.3	-	23.1	-	-	5.72	-	-	11.7	-	-	22.8	-
2.4	-	24.7	-	-	5.65	-	-	11.7	-	-	23.8	-
2.5	-	23.3	-	-	6.58	-	-	9.6	-	-	22.4	-
2.6	-	20.6	-	-	5.21	-	-	7.8	-	-	18.8	-
2.7	-	13.4	-	-	5.98	-	-	5.5	-	-	14.6	-

2.8	-	8.5	-	-	5.02	-	-	4.1	-	-	8.5	-
3.1	-	-	22.6	-	-	5.59	-	-	9.9	-	-	22.7
3.2	-	-	23.5	-	-	7.62	-	-	10.4	-	-	23.4
3.3	-	-	23.5	-	-	8.41	-	-	9.8	-	-	22.4
3.4	-	-	23.0	-	-	7.69	-	-	9.8	-	-	21.4
3.5	-	-	21.1	-	-	8.40	-	-	7.4	-	-	17.1
3.6	-	-	19.6	-	-	5.30	-	-	8.1	-	-	16.5
3.7	-	-	15.2	-	-	4.49	-	-	7.1	-	-	13.6
3.8	-	-	11.5	-	-	4.55	-	-	4.4	-	-	9.7
3.9	-	-	31.2	-	-	6.72	-	-	13.0	-	-	44.4
3.10	-	-	23.3	-	-	11.71	-	-	8.2	-	-	21.3
3.11	-	-	21.0	-	-	8.83	-	-	7.1	-	-	19.2
3.12	-	-	17.2	-	-	5.76	-	-	5.3	-	-	17.4
3.13	-	-	27.2	-	-	7.59	-	-	12.5	-	-	26.3
3.14	-	-	26.2	-	-	11.29	-	-	8.0	-	-	21.1
3.15	-	-	20.9	-	-	8.78	-	-	6.9	-	-	18.7
3.16	-	-	13.6	-	-	5.76	-	-	5.1	-	-	16.2